

Less noticeable shallow decay phase in early X-ray afterglows of GeV/TeV-detected gamma-ray bursts

Ryo Yamazaki,^{1*} Yuri Sato¹, Takanori Sakamoto¹, Motoko Serino¹

¹*Department of Physics and Mathematics, Aoyama Gakuin University, 5-10-1 Fuchinobe, Sagami-hara 252-5258, Japan*

ABSTRACT

The nature of the shallow decay phase in the X-ray afterglow of the gamma-ray burst (GRB) is not yet clarified. We analyze the data of early X-ray afterglows of 26 GRBs triggered by Burst Alert Telescope onboard *Neil Gehrels Swift Observatory* and subsequently detected by *Fermi* Large Area Telescope and/or ground-based atmospheric Cherenkov telescopes. It is found that 9 events (including 2 out of 3 very-high-energy gamma-ray events) have no shallow decay phase and that their X-ray afterglow light curves are well described by single power-law model except for the jet break at later epoch. The fraction of such events is significantly larger than the value (about 5%) for all long GRBs detected by X-ray Telescope onboard *Swift*. The rest are fitted by double power-law model and have a break in the early epoch (around ks), however, 8 events (including a very-high-energy gamma-ray event) have the pre-break decay index larger than 0.7. Therefore, a large fraction of GRBs detected in high-energy and very-high-energy gamma-ray bands has no shallow decay phase, or they have less noticeable shallow decay phase in the early X-ray afterglow. A possible interpretation along with the energy injection model is briefly discussed.

Key words: (transients:) gamma-ray bursts — (stars:) gamma-ray burst: general

1 INTRODUCTION

X-ray afterglows of gamma-ray bursts (GRBs) are not fully understood as of yet (see, e.g., Kumar & Zhang 2015, for review). Their canonical behavior consists of the initial steep decay phase, the shallow decay phase and the normal decay phase (Nousek, et al. 2006; Zhang, et al. 2006), which is subsequently followed by the steepening again due to the jet break (Liang, et al. 2008; Racusin, et al. 2009). The initial steep decay phase is most likely the tail emission of the prompt GRB (Kumar & Panaitescu 2000; Zhang, et al. 2006; Yamazaki, et al. 2006), and the late normal decay phase is well explained by the external forward shock model proposed in the pre-*Swift* era (Sari, Piran & Narayan 1998). The most enigmatic is the shallow decay phase which typically lasts 10^{3-4} s (Willingale, et al. 2007; Liang, Zhang & Zhang 2007; Sakamoto, et al. 2008; Dainotti, et al. 2010, 2013, 2016; Margutti, et al. 2013; Tang et al. 2019; Zhao et al. 2019). Proposed models are the energy injection model (Nousek, et al. 2006; Zhang, et al. 2006; Granot & Kumar 2006; Kobayashi & Zhang 2007), the inhomogeneous or two-component jet model (Toma, et al. 2006; Eichler & Granot

2006; Granot, Königl & Piran 2006; Beniamini et al. 2019), the time-dependent microphysics model (Ioka, et al. 2006; Granot, Königl & Piran 2006; Fan & Piran 2006), the prior explosion model (Ioka, et al. 2006; Yamazaki 2009), the cannonball model (Dado, Dar & De Rújula 2006), the reverse shock-dominated afterglow model (Genet, Daigne & Mochkovitch 2007), the internal engine model (Ghisellini, et al. 2007), the super-critical pile model (Sultana, Kazanas & Mastichiadis 2013), the collapsar model ejecting thick shells (van Eerten 2014), and so on. To clarify the mechanism of the shallow decay phase, additional observational information other than X-rays is necessary.

High-energy gamma-ray emissions are detected by *Fermi* Large Area Telescope (LAT) either during or after the prompt GRB emission, origin of which is still under debate (see Nava 2018, for review). The early emission detected in the prompt phase may have an internal origin, and comes from leptonic inverse Compton process with various seed photons (Bošnjak, Daigne & Dubus 2009; Zhang, et al. 2011; Toma, Wu & Mészáros 2011; Asano & Mészáros 2012; Daigne 2012; Oganessian, et al. 2017) or from hadronic process (Asano, Inoue & Mészáros 2009; Asano & Mészáros 2012; Razzaque, Dermer & Finke 2010). The temporally extended emission is likely the afterglow synchrotron emis-

* E-mail: ryo@phys.aoyama.ac.jp (RY)

sion arising in the external shock (Kumar & Barniol Duran 2009, 2010; Ghisellini, et al. 2010; Nava, et al. 2014). Recently, ground-based atmospheric Cherenkov telescopes, the Major Atmospheric Gamma Imaging Cherenkov (MAGIC) telescopes and the High Energy Stereoscopic System (H.E.S.S.), detected very-high-energy (VHE) gamma-rays from GRB 180720B (Roberts & Meegan 2018; Ruiz-Velasco 2019), GRB 190114C (Ajello et al. 2019b; Mirzoyan 2019) and GRB 190829A (Fermi GBM collaboration 2019; de Naurois 2019). The VHE gamma-rays are most likely synchrotron self-Compton emission (Wang, et al. 2019; Derishev & Piran 2019; Fraija et al. 2019). It is expected that in near future the number of such *VHE events* rapidly increases when Cherenkov Telescope Array (CTA) starts observations of GRBs (Kakuwa, et al. 2012; Inoue, et al. 2013; Gilmore, et al. 2013). VHE gamma-ray observations with CTA may even provide a clue to the origin of shallow decay phase in the X-ray afterglow (e.g., Murase, et al. 2010, 2011).

At present, a link between the X-ray shallow decay phase and (very-)high-energy gamma-ray emission is unclear. It is known that the LAT-detected GRBs are among the most energetic GRBs (Ackermann, et al. 2013; Atteia, et al. 2017; Nava, et al. 2014; Ajello et al. 2019a), so that their kinetic energy of the GRB jet is larger than usual events without high-energy gamma-ray detection. There is also an observational implication that the initial bulk Lorentz factor of the jet is larger for LAT-detected GRBs (Ghirlanda, et al. 2012). Furthermore, emission region of the high-energy gamma-rays might have smaller magnetic field energy density (Tak, et al. 2019). Hence one can expect that their outflow has different characteristics, so that the X-ray afterglow behaves differently. Therefore, studies of the X-ray afterglow of such extreme GRBs may provide us hints for unveiling the nature of the shallow decay phase.

In this paper, as a first step of investigating connection between the shallow decay phase and the high-energy (and VHE) gamma-ray emission, we analyze early X-ray afterglows of GRBs with detected high-energy and VHE gamma-rays. We find that their decay slopes of the shallow decay phase tends to be steeper than GRBs without high-energy/VHE gamma-ray detection, so that the X-ray shallow decay phase looks less noticeable. This fact has been already noted in previous literature very briefly (Kumar & Zhang 2015). Present work provides analysis result more quantitatively with better statistics due to larger sample size.

2 SAMPLE SELECTION

In this paper, we analyze early X-ray afterglows of GRBs which are listed in the second catalog of LAT-detected GRBs (Ajello et al. 2019a). The catalog includes 186 events covering from 2008 to 2018 August 4. There are 24 events in the catalog which were triggered by Burst Alert Telescope (BAT) onboard *Swift* and subsequently observed by X-ray Telescope (XRT) typically ~ 100 s after the burst onset. Among them, XRT data of GRB 170813A consists of only 4 data points after the initial steep decay phase, so that we remove this event from our sample in order to consider well-sampled early X-ray afterglow light curves.

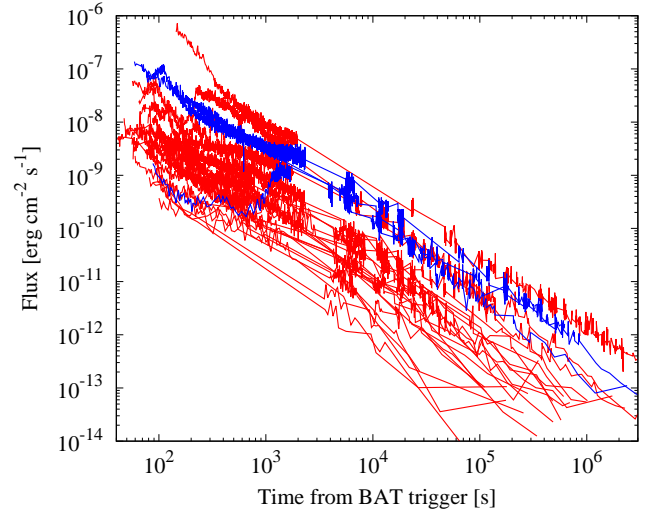


Figure 1. X-ray afterglow light curves of 26 events in our sample, which consists of 23 events which is listed in the second catalog of LAT-detected GRBs (red curves) and 3 VHE events (blue lines).

So far VHE gamma-rays from 3 GRBs (GRB 180720B, 190114C, and 190829A) are detected by MAGIC and H.E.S.S. (Ruiz-Velasco 2019; Mirzoyan 2019; de Naurois 2019). Fortunately all are triggered by *Swift*/BAT, so that early X-ray afterglows are observed by XRT. Hence we analyze XRT data of these events.

All events of our sample are listed in Table 1, and their X-ray light curves are shown in Fig. 1. It contains 26 GRBs (23 LAT GRBs + 3 VHE events) in total. Tang et al. (2019) and Zhao et al. (2019) collected 174 and 201 GRBs with clear shallow decay phase, respectively. Within our present sample, only 4 events (GRB 090510, 110213A, 150403A and 180720B) overlaps with the list of the former, and 3 events (GRB 090102, 090510 and 140323A) overlaps with the latter. This fact already shows that there are less events hosting typical shallow decay phase in our present sample.

Finally we note that our sample contains a short GRB 090510. The other events are long GRBs.

3 DATA ANALYSIS

The *Swift*/XRT data were downloaded from the *Swift* team website¹ (Evans et al. 2007, 2009). First the X-ray light curves in the time interval $[t_1, t_2]$ is fitted with single power-law (SPL) function,

$$f_S(t) = f_0 t^{-\alpha_1}, \quad (1)$$

where f_0 and α_1 are a normalization constant and a decay slope, respectively. We choose the time interval $[t_1, t_2]$ excluding the steep decay phase and X-ray flares if they exist. Subsequently, we also fit the light curves with double power-law (DPL) function,

$$f_D(t) = f_0 [(t/t_b)^{\alpha_1} + (t/t_b)^{\alpha_2}]^{-1/w}, \quad (2)$$

with α_1 and α_2 describing the decay slopes of pre-

¹ https://www.swift.ac.uk/xrt_curves/

Table 1. Best-fit model parameters of GRBs in our sample.

GRB	t_1-t_2 [ks]	SPL model : $f_S(t)$		DPL model: $f_D(t)$			$\Delta\chi^2$ ^a	
		α_1	χ^2/dof	α_1	α_2	t_b [ks]		χ^2/dof
Single power law (SPL) events								
081203A	0.1–30	1.31 ± 0.02	1590/297					< 1
110625A	0.1–20	1.14 ± 0.03	90/53					< 1
121011A	0.08–12	1.48 ± 0.03	38/19					< 1
151006A	0.1–100	1.40 ± 0.01	159/157					< 1
170405A	0.2–10	1.40 ± 0.03	818/206					< 1
Double power law (DPL) events								
090102	0.3–45	1.29 ± 0.01	143/121	0.21 ± 0.36	1.37 ± 0.03	0.62 ± 0.11	111/119	32
090510 ^b	0.07–20	1.07 ± 0.05	460/70	0.64 ± 0.05	2.11 ± 0.12	1.46 ± 0.23	103/68	357
100728A	0.8–1000	1.26 ± 0.01	621/295	1.14 ± 0.04	1.65 ± 0.06	16.5 ± 6.88	499/293	122
110213A	0.15–1000	1.23 ± 0.03	2069/232	0.04 ± 0.06	1.82 ± 0.03	3.26 ± 0.17	400/230	1669
110731A	0.09–100	1.16 ± 0.01	346/268	1.13 ± 0.02	1.72 ± 0.22	25.1 ± 8.37	332/266	15
120729A ^c	0.05–40	1.18 ± 0.02	329/113	1.11 ± 0.02	2.82 ± 0.38	8.03 ± 1.38	202/111	128
130427A	0.35–1000	1.277 ± 0.003	2374/1409	1.18 ± 0.06	1.34 ± 0.04	3.97 ± 10.9	2335/1407	39
130907A	0.22–100	1.456 ± 0.004	4125/2296	1.36 ± 0.03	1.60 ± 0.05	5.80 ± 6.33	3937/2294	189
140102A	0.04–10	1.15 ± 0.01	804/524	1.05 ± 0.02	1.55 ± 0.07	1.71 ± 0.51	668/522	137
140323A	0.2–100	0.82 ± 0.02	551/112	0.60 ± 0.03	1.67 ± 0.10	10.2 ± 1.76	184/110	367
150314A	0.09–11	1.03 ± 0.01	1015/641	0.90 ± 0.01	1.47 ± 0.03	2.32 ± 0.36	951/672	65
150403A	0.2–100	1.04 ± 0.01	6385/1601	0.43 ± 0.02	1.27 ± 0.01	1.28 ± 0.07	1813/1599	4572
160325A	0.2–10	1.36 ± 0.02	202/128	0.98 ± 0.29	1.53 ± 0.11	0.45 ± 0.47	182/126	20
160905A	0.1–100	0.96 ± 0.01	3796/989	0.66 ± 0.02	1.35 ± 0.02	1.48 ± 0.14	1495/987	2301
160917A ^c	0.07–25	1.25 ± 0.02	52.4/32	1.22 ± 0.03	2.33 ± 0.72	12.2 ± 4.25	42.2/30	10.2
170728B	0.3–20	0.99 ± 0.01	374/196	0.32 ± 0.17	1.22 ± 0.03	1.21 ± 0.32	275/194	99
170906A	0.2–30	1.26 ± 0.03	2055/267	0.35 ± 0.05	1.91 ± 0.14	1.14 ± 0.30	450/265	1605
171120A	3–150	0.61 ± 0.04	173/75	0.39 ± 0.06	1.77 ± 0.24	37.0 ± 8.2	87/73	85
Very-high-energy gamma-ray (VHE) events								
180720B	0.25–100	0.931 ± 0.004	7233/3361	0.74 ± 0.01	1.43 ± 0.02	4.70 ± 0.23	4731/3359	2502
190114C	0.065–100	1.338 ± 0.004	1822/1030					< 1
190829A	2–100	1.33 ± 0.02	451/235					< 1

Notes.
^a A DPL model is statistically preferred at $> 3\sigma$ over a simpler SPL model when $\Delta\chi^2 > 10$.

^b A short GRB.

^c Best-fit values of α_1 and α_2 of DPL model are consistent with the jet break (see section 5).

and post-break segments, respectively, and t_b is a break time. A smoothness parameter w is fixed to be 3 (Liang, Zhang & Zhang 2007; Zhao et al. 2019).

We compare above two models in order to determine whether the additional degrees of freedom in the DPL model are warranted over a simpler SPL model. We fit all light curves of 26 events with both models and obtain χ^2 of the best-fitted parameter set. Then, the difference between χ^2 of the two models, $\Delta\chi^2$, is calculated for our 26 bursts. Since there are two additional free parameters between the two models, a value of $\Delta\chi^2 > 10$ would represent a $> 3\sigma$ improvement in the fit. We adopt this criterion as the threshold for a statistical preference for a break in the light curve.

4 RESULTS

The results of the analysis on 26 events in our sample are shown in Table 1. The upper most 5 events in the table are fitted with both SPL and DPL models, however, we find $\Delta\chi^2 < 1$, so that additional two parameters of the DPL model do not improve the fit. We call them *SPL events*. The other events in the table except for the lowest three VHE events have $\Delta\chi^2 > 10$, so that the DPL model is statistically preferred at $> 3\sigma$ over SPL model. Hence, they are named as *DPL events* in this paper. We also analyze 3 VHE events in

a similar manner, and find that two events (GRB 190114C and 190829A) are fitted with the SPL model and that the other one (GRB 180720B) is described by the DPL model.

Figure 2 shows the distribution of α_1 for 5 SPL and 18 DPL events. For the DPL events we take the best-fitted values of α_1 of the DPL model rather than the SPL model. The two Gaussian distributions (dashed and dotted lines) are taken from Tang et al. (2019) and Zhao et al. (2019), describing the distribution of the temporal index of the shallow decay phase. Although the statistics is poor, our 26 events (including VHE events shown by arrows) tend to have larger value of α_1 than those with typical shallow decay phase. It is also noted that the SPL events sit the upper end of the α_1 distribution. If $\alpha_1 > 1$, the decay phase is no longer the shallow decay phase, but the normal decay phase.

To see the decay properties of the DPL events in more detail, we show in Figure 3 the best-fitted parameters (α_1 , α_2 and t_b) of DPL events in the α_1-t_b (left panel) and $\alpha_1-\alpha_2$ planes (right panel). Grey points are those with clear shallow decay phase whose data are taken from Tang et al. (2019). It is found from Fig. 3 that compared with events of Tang et al. (2019), roughly a half of our 18 events with a VHE event has larger pre-break decay index α_1 while the break time t_b and the post-break decay index α_2 of our sample are roughly similar to those of Tang et al. (2019).

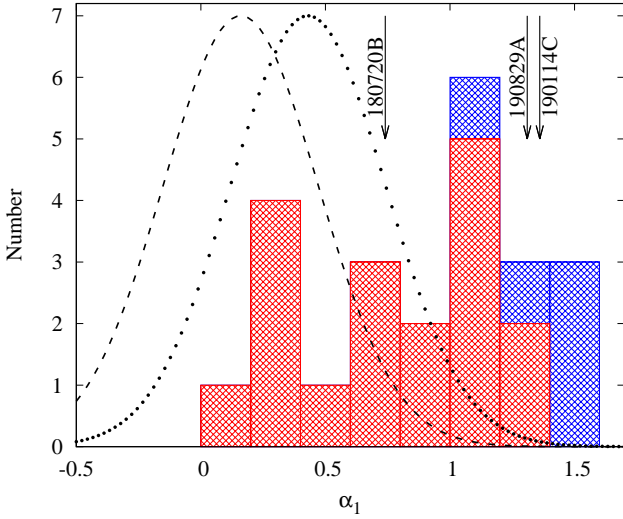


Figure 2. Blue and red histograms show the distributions of the decay slope α_1 for 5 SPL and 18 DPL events, respectively. Dashed and dotted lines are those for long GRBs with typical shallow decay phase taken from Tang et al. (2019) and Zhao et al. (2019), respectively. Also shown are arrows describing the values of α_1 for 3 VHE events.

According to these results, we schematically draw in Fig. 4 the typical behavior of GRBs in our sample.

5 DISCUSSION

In the α_1 - α_2 plane for DPL events, there are two data points (GRB 120729 and 160917A) whose best-fit values $\alpha_1 > 1$ and $\alpha_2 > 2$. Although the break time $t_b \sim 10^4$ s for these bursts, the measured break should be taken as a jet break rather than the *shallow-to-normal* break. According to the theory of the jet break, if the X-ray afterglow is in the slow cooling regime with the X-ray band frequency larger than the cooling frequency ν_c , then the decay indices are given by $(3p - 2)/4$ and p for pre- and post-jet break, respectively, where p is an index of the power-law electron distribution (Sari, Piran & Halpern 1999). For GRB 160917A, if the measured value of $\alpha_1 = 1.22 \pm 0.03$ corresponds to the pre-jet break decay index, then we have $p = (2 + 4\alpha_1)/3 = 2.29 \pm 0.04$, so that the observed value of $\alpha_2 = 2.33 \pm 0.72$ is consistent with the post-jet break decay index within 1σ error. On the other hand, GRB 120729A may not follow the jet break theory. Similar calculation for GRB 120729A leads to $p = (2 + 4\alpha_1)/3 = 2.15 \pm 0.03$, which is somewhat smaller than the measured post-break index $\alpha_2 = 2.82 \pm 0.38$ but still consistent within 2σ error. Nevertheless, the post-break decay index α_2 is too steep for the normal decay phase of the X-ray afterglow. Therefore, these bursts should be treated as events without shallow decay phase.

Taking into account the correction described in the previous paragraph, we calculate the fraction of events without shallow decay phase as 5 SPL as well as 2 DPL events (GRB 120729 and 160917A) for 23 events, so that $7/23 \approx 30\%$. This fraction is significantly larger than the value of

$19/400 \approx 5\%$ for all long GRBs with XRT detection from 2005 January to 2009 July (Liang, et al. 2009). Furthermore, two (GRB 190114C and 190829A) out of 3 VHE events have no shallow decay phase. Even if X-ray light curve has a break at t_b , eight events (GRB 100728A, 110731A, 130427A, 130907A, 140102A, 150314A, 160325A and a VHE event GRB 180720B) have the pre-break decay index α_1 larger than 0.7. For the sample of Zhao et al. (2019), the distribution of the pre-break decay index has a mean of 0.43 and a dispersion of 0.22 (see dotted line in Fig. 2), hence the 8 events with $\alpha_1 > 0.7$ deviate from the mean value for ordinary GRBs more than 1σ . Hence one can say that a large fraction (17 out of 26 events) of GRBs detected in high-energy and VHE gamma-ray bands has no shallow decay phase, or they have less noticeable shallow decay phase in the early X-ray afterglow.

Our present result may constrain models of the shallow decay phase of the X-ray afterglow. In the context of the energy injection model (Nousek, et al. 2006; Zhang, et al. 2006; Granot & Kumar 2006; Kobayashi & Zhang 2007), initial outflow energy is small, so that the X-ray afterglow arising from the external shock is initially dim. If the additional energy is injected to the flow, then the X-ray afterglow becomes brighter than that in the case of no energy injection, resulting in the shallow decay phase. For high-energy gamma-ray events, isotropic gamma-ray energy of the prompt emission is larger (Ackermann, et al. 2013; Atteia, et al. 2017; Nava, et al. 2014; Ajello et al. 2019a), hence it is expected that the initial outflow energy is also large. In this case, the X-ray afterglow is already bright from the beginning, and it shows no shallow decay phase. Therefore, this model naturally explains the present result that a large fraction of events of our sample have no clear shallow decay phase. Some other models will be challenged if more data are accumulated in future.

We also search for any correlation between X-ray light curve parameters like α_1 and t_b and GeV properties listed in the second catalog of LAT-detected GRBs (Ajello et al. 2019a), such as the temporal decay index α_{GeV} , spectral index β , and isotropic energy of the gamma-ray emission in the LAT energy band E_{iso} . Among 2 (α_1 and t_b) \times 3 (α_{GeV} , β and E_{iso}) = 6 combinations, we find no statistically significant correlation because of small sample size. More events are necessary to have larger sample, and further analysis with better statistics is left for future work.

ACKNOWLEDGMENTS

We would like to thank Drs. K. Asano, K. Ioka and S. J. Tanaka for valuable comments to improve this paper. This work made use of data supplied by the UK Swift Science Data Centre at the University of Leicester. This work is supported in part by grant-in-aid from the Ministry of Education, Culture, Sports, Science, and Technology (MEXT) of Japan, No.18H01232(RY), No.17H06362(TS), No.18H01257(TS), and No.17K05402(MS).

Facility: Swift and Fermi.

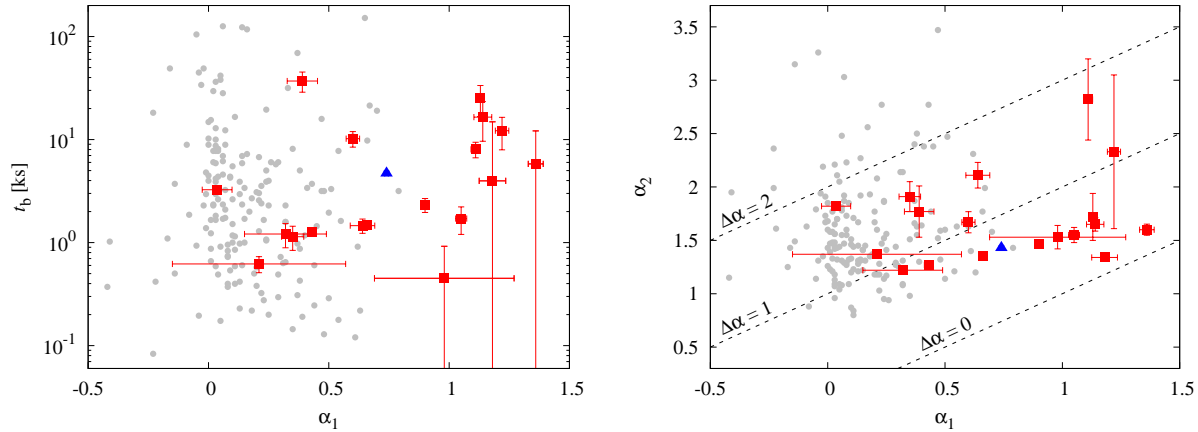


Figure 3. Comparison of our 18 DPL events (red squares) and a VHE event (GRB 180720B: blue triangle) to bursts with typical shallow decay phase (grey dots: taken from Tang et al. 2019) in α_1 - t_b plane (left panel) and α_1 - α_2 plane (right panel).

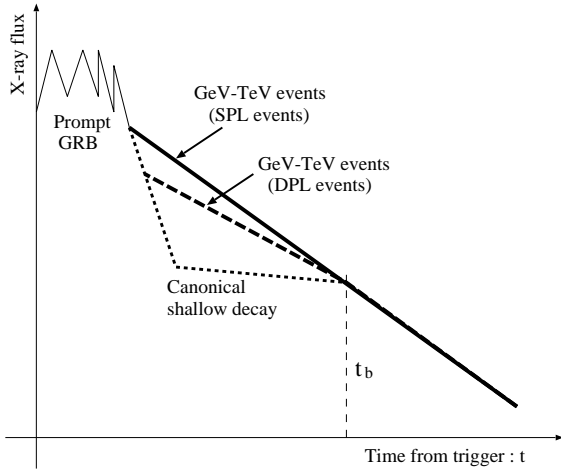


Figure 4. Schematic view of early X-ray afterglow light curves of events considered in this paper. Five SPL and 2 DPL events (GRB120729 and 160917A) have no shallow decay phase. Seven DPL and a VHE events have $\alpha_1 > 0.7$, so that the decay slope before the break time t_b is somewhat steeper than typical shallow decay phase.

REFERENCES

- Ackermann M., et al., 2013, *ApJS*, 209, 11
 Ajello M., et al., 2019a, *ApJ*, 878, 52
 Ajello M., et al., 2019b, preprint (arXiv:1909.10605)
 Asano K., Inoue S., Mészáros P., 2009, *ApJ*, 699, 953
 Asano K., Mészáros P., 2012, *ApJ*, 757, 115
 Atteia J.-L., et al., 2017, *ApJ*, 837, 119
 Beniamini P. et al. 2019, preprint (arXiv:1907.05899)
 Bošnjak Ž., Daigne F., Dubus G., 2009, *A&A*, 498, 677
 Dado S., Dar A., De Rújula A., 2006, *ApJL*, 646, L21
 Daigne F., 2012, *IJMPS*, 8, 196
 Dainotti M. G., Willingale R., Capozziello S., Fabrizio Cardone V., Ostrowski M., 2010, *ApJL*, 722, L215
 Dainotti M. G., Petrosian V., Singal J., Ostrowski M., 2013, *ApJ*, 774, 157
 Dainotti M. G., Postnikov S., Hernandez X., Ostrowski M., 2016, *ApJL*, 825, L20

- de Naurois M. (H. E. S. S. Collaboration), 2019, *The Astronomer’s Telegram*, 13052
 Derishev E. & Piran, T., 2019, preprint (arXiv:1905.08285)
 Eichler D., Granot J., 2006, *ApJL*, 641, L5
 Evans P. A., Beardmore A. P., Page K. L., et al. 2007, *A&A*, 469, 379
 Evans P. A., Beardmore A. P., Page K. L., et al. 2009, *MNRAS*, 397, 1177
 Fan Y., Piran T., 2006, *MNRAS*, 369, 197
 Fermi GBM collaboration, 2019, *GRB Coordinates Network*, 25551
 Fraija N., et al., 2019, preprint (arXiv:1907.06675)
 Genet F., Daigne F., Mochkovitch R., 2007, *MNRAS*, 381, 732
 Ghirlanda G., Nava L., Ghisellini G., Celotti A., Burlon D., Covino S., Melandri A., 2012, *MNRAS*, 420, 483
 Ghisellini G., Ghirlanda G., Nava L., Celotti A., 2010, *MNRAS*, 403, 926
 Ghisellini G., Ghirlanda G., Nava L., Firmani C., 2007, *ApJL*, 658, L75
 Gilmore R. C., Bouvier A., Connaughton V., Goldstein A., Otte N., Primack J. R., Williams D. A., 2013, *ExA*, 35, 413
 Granot J., Königl A., Piran T., 2006, *MNRAS*, 370, 1946
 Granot J., Kumar P., 2006, *MNRAS*, 366, L13
 Inoue S., et al., 2013, *APh*, 43, 252
 Ioka K., Toma K., Yamazaki R., Nakamura T., 2006, *A&A*, 458, 7
 Kakuwa J., Murase K., Toma K., Inoue S., Yamazaki R., Ioka K., 2012, *MNRAS*, 425, 514
 Kobayashi S., Zhang B., 2007, *ApJ*, 655, 973
 Kumar P., Barniol Duran R., 2009, *MNRAS*, 400, L75
 Kumar P., Barniol Duran R., 2010, *MNRAS*, 409, 226
 Kumar P., Panaitescu A., 2000, *ApJL*, 541, L51
 Kumar P., Zhang B., 2015, *PhR*, 561, 1
 Liang E.-W., Zhang B.-B., Zhang B., 2007, *ApJ*, 670, 565
 Liang E.-W., Racusin J. L., Zhang B., Zhang B.-B., Burrows D. N., 2008, *ApJ*, 675, 528
 Liang E.-W., Lü H.-J., Hou S.-J., Zhang B.-B., Zhang B., 2009, *ApJ*, 707, 328
 Mirzoyan R. (MAGIC Collaboration), 2019, *The Astronomer’s Telegram*, 12390

- Margutti R., et al., 2013, MNRAS, 428, 729
- Murase K., Toma K., Yamazaki R., Nagataki S., Ioka K., 2010, MNRAS, 402, L54
- Murase K., Toma K., Yamazaki R., Mészáros P., 2011, ApJ, 732, 77
- Nava L., et al., 2014, MNRAS, 443, 3578
- Nava L., 2018, IJMPD, 27, 1842003
- Nousek J. A., et al., 2006, ApJ, 642, 389
- Oganesyan G., Nava L., Ghirlanda G., Celotti A., 2017, ApJ, 846, 137
- Racusin J. L., et al., 2009, ApJ, 698, 43
- Razzaque S., Dermer C. D., Finke J. D., 2010, OAJ, 3, 150
- Roberts, O. J. & Meegan, C. 2018, GRB Coordinates Network, 22981
- Ruiz-Velasco, E. L. 2019, 1st International Cherenkov Telescope Array Symposium, Bologna, 6-9 May 2019
- Sakamoto T., et al., 2008, ApJ, 679, 570
- Sari R., Piran T., Narayan R., 1998, ApJL, 497, L17
- Sari R., Piran T., Halpern J. P., 1999, ApJL, 519, L17
- Sultana J., Kazanas D., Mastichiadis A., 2013, ApJ, 779, 16
- Tak D., Omodei N., Uhm Z. L., Racusin J., Asano K., McEnery J., 2019, ApJ, 883, 134
- Tang C.-H. et al. 2019, preprint (arXiv:1905.07929)
- Toma K., Ioka K., Yamazaki R., Nakamura T., 2006, ApJL, 640, L139
- Toma K., Wu X.-F., Mészáros P., 2011, MNRAS, 415, 1663
- van Eerten H. J., 2014, MNRAS, 445, 2414
- Wang X.-Y., Liu R.-Y., Zhang H.-M., Xi S.-Q., Zhang B., 2019, arXiv, arXiv:1905.11312
- Willingale R., et al., 2007, ApJ, 662, 1093
- Yamazaki R., Toma K., Ioka K., Nakamura T., 2006, MNRAS, 369, 311
- Yamazaki R., 2009, ApJL, 690, L118
- Zhang B., et al., 2006, ApJ, 642, 354
- Zhang B.-B., et al., 2011, ApJ, 730, 141
- Zhao L. et al. 2019, ApJ, 883, 97